EUSIPCO 2013 1569746251

ACOUSTIC SOUND SOURCE TRACKING FOR A MOVING OBJECT USING PRECISE DOPPLER-SHIFT MEASUREMENT

Suminori Nishie, Masato Akagi

School of Information Science, Japan Advanced Institute of Science and Technology (JAIST)
1-1 Asahidai, Nomi, Ishikawa, 923-1292, Japan
{snishie, akagi }@jaist.ac.jp

ABSTRACT

We propose a sound source tracking method for a moving object that precisely measures the Doppler-shifted frequency. In order to track a moving sound source by determining velocity and location, it is necessary to measure the precise frequency shift in real time. On the other hand, in sonar signal processing, the Doppler shift estimation is used for moving targets localization. This amount is measured indirectly, mostly by using the Kalman filter or other modern particle filters. However, such filters require a complicated estimation process. Considering such a drawback in measuring the Doppler-shift measurement, our method directly measures the Doppler-shifted frequency without the Fourier transform or Kalman filter. In order to verify the effectiveness of our method, we evaluated the frequency resolution and the precision and the noise robustness of our method. Experimental results show that our method can detect the precise Doppler-Shift of moving sound source. We discuss the estimation data of the location/velocity of a moving sound source. We also discuss the advanced frequency tracking capability of our method.

Index Terms— Doppler Effect, Phase Difference, Lissajous' Figure, Comb Filter, Weierstrass Substitution

1. INTRODUCTION

For making sound tracking of a moving object possible, it is necessary to measure the Doppler-shifted frequency in real time. Therefore, we propose a novel method for precise frequency measurement.

Our method does not use the Fourier Transform (FFT) / Short Time Fourier Transform (STFT) or an estimation process such as the Kalman filter. Using the FFT has a time-frequency resolution limitation of $|\Delta\omega||\Delta t| \geq 1/2$. For moving sound source tracking, less than 1 Hz in frequency shift must be measured in a short time; therefore, using the FFT is not suitable. The Kalman-filter is a typical implementation [1] for tracking the frequency movement of targets in sonar signal processing. The use of other modern particle filters [2][3] has also been reported. However, using the Kalman filter essentially results in an estimation error. Based on such a background, we developed a method for precise frequency measurement, which also involves precise measurement of the phase difference of two signals. We call this method Primary Rotation and Instantaneous Movement Observation (PRIMO), which can directly measure the precise frequency and phase difference. The required and established frequency resolution is in the order of 10^{-3} Hz. This capability may replace traditional Doppler-shift measurement.

The goal of this research is to develop essential core methods for precisely measuring the Doppler-shifted frequency on moving sound source tracking. To simplify the experiment and evaluation, we used two microphones and a fixed sound source frequency model. We measured the phase difference between the two microphones instead of actual location tracking. We show the fundamental time-frequency resolution capability of our method, by evaluating the calibration and the noise robustness. The experimental results indicate that PRIMO is effective in sound source tracking.

This paper explains the principle of PRIMO, and proposes a sound source tracking method for a moving object, using PRIMO, for precise Doppler-shifted frequency measurement.

2. PRINCIPLE OF DOPPLER-SHIFT MEASUREMENT

This section describes the principle of PRIMO. In this paper, we use the normalized frequency $F = \frac{f}{fs}$ and the normalized angular frequency $\Omega = 2\pi F$ representation, where f_s is the sampling frequency. Let ϕ denote phase difference in this paper.

2.1. Frequency Measurement Overview

The signal processing diagram for the Doppler shift measurement is shown in Fig.1. The PRIMO diagram involves the three following major calculating steps.

1. The first step processes the input signal by using an IIR-type comb filter. The signal passes only around the resonant frequencies. An enlarged phase difference between the input and output signals is generated.
2. The second step involves precise phase difference measurement between the input and output of the comb filter. This measurement step was devised to be more accurate based on a traditional Lissajous' figure, which focuses on the instantaneous partial area caused by the trajectory movement.
3. The third step is frequency estimation without approximation, which involves calculating the original frequency deviation from the given phase difference using the inverse phase transfer function. The Weierstrass substitution is used for the solution.
4. Through these three steps, a small frequency deviation around the resonant frequency can be precisely estimated, at least in the order of 10^{-3} Hz.

2.2. Frequency-Phase Transform by Using the Comb Filter

This section describes a phase shift characteristic naturally generated by the IIR-type comb filter behaving as an "Frequency-Phase Transform". The IIR-type comb-filter is illustrated in Fig.2 (A). The parameter K represents the delay count and a is the feedback gain with $|a|<1$. The transfer function is given by Eq.(1) with the normalized

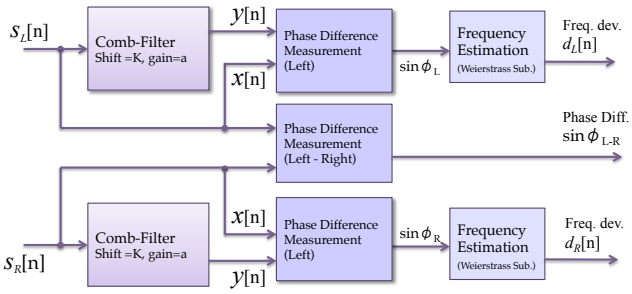

Fig. 1. Signal Processing Diagram for 2CH inputs.

angular frequency Ω. Note that the angular frequency $\Omega = \pi$ is the Nyquist frequency in the discrete system. Parameter a is important to determine the desired phase shift characteristic. The resonant frequency is determined as $f_0 = \frac{f_s}{2K}$ or $F_0 = \frac{1}{2K}$.

$$H(\Omega)=\frac{1}{(1+a^2)-2a\cos(\Omega K)}\{1-a\cos(\Omega K)-ja\sin(\Omega K)\} \quad (1)$$

The value of the gain parameter a is required to be negative with $-1<a<0$. This ensures the resonant frequency for odd harmonics. From the transfer function $H(\Omega)$, the phase transfer function $\phi(\Omega)$

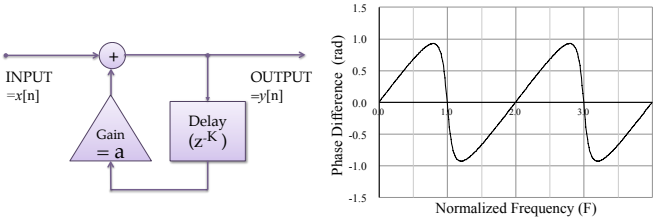

(A) IIR Comb Filter (b) Phase Transfer Function (a=-0.8)

Fig. 2. The IIR Comb-Filter.

can be obtained as:

$$\tan(\phi(\Omega)) = \frac{Im(H)}{Re(H)} = \frac{-a\sin(\Omega K)}{1-a\cos(\Omega K)} \quad (2)$$

PRIMO intends to utilize the steep change on the resonant frequency.

2.3. Measuring the Phase Difference

This section describes the calculation of the phase difference. The Lissajous' figure is traditionally well known [4] for phase difference measurement in electric/electronic engineering. This step involves an improved operation compared with the original traditional Lissajous' figure operation. First, we focus on the total area of the Lissajous' figure using closed curve integration. The area of the closed curve S is expressed by Eq.(3), where T is the fundamental period.

$$S = \frac{1}{2}\oint_0^T \{x\cdot\frac{dy}{dt} - y\cdot\frac{dx}{dt}\}dt \quad (3)$$

Equation (3) can be obtained involving Green's Theorem by Eq.(4), where $P=-y, Q=x$.

$$\oint_C \{Pdx+Qdy\} = \iint_D \{\frac{\partial Q}{\partial x} - \frac{\partial P}{\partial y}\}dxdy \quad (4)$$

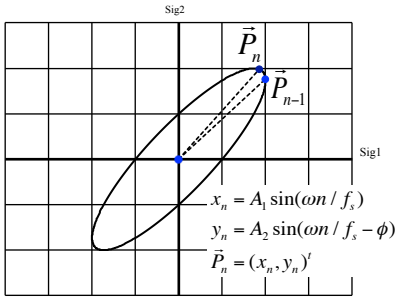

Fig. 3. Lissajous' Figure for Phase Angle Calculation

PRIMO focuses on the partial area bounded by two trajectory locations P_{n-1}, P_n, on the Lissajous' figure. First, let the signals be given by following equation, where ϕ is phase difference.

$$x(t) = A_1\sin(\omega t), \quad y(t) = A_2\sin(\omega t - \phi) \quad (5)$$

If the current time t is given, we can obtain the amount of the area bounded by the two signals $x(t), y(t)$ as:

$$S(t) = \frac{1}{2}\int_0^t \{x\frac{dy}{d\tau} - y\frac{dx}{d\tau}\}d\tau \quad (6)$$

The differentiation $\frac{d}{dt}S(t)$ is given by Eq.(7), which shows the change of the area. Note that this becomes constant.

$$\frac{d}{dt}S(t) = \frac{1}{2}A_1A_2\omega\sin\phi \quad (7)$$

From here, we focus on the discrete domain. If we assume a short period Δt, we can obtain the small partial area ΔS as Eq.(8).

$$\Delta S = \frac{d}{dt}S(t)\Delta t \quad (8)$$

We use vector representation to show the current trajectory location as shown in Fig.3. $\vec{P_n}$ is a pair of instantaneous values of x_n and y_n in the discrete domain.

$$\vec{P_n} = [x_n, y_n]^t \quad (9)$$

Considering we can easily obtain ΔS if we using the vector cross product of P_{n-1}, with P_n.

$$\Delta S = \frac{1}{2}|\vec{P_{n-1}}\times\vec{P_n}| \quad (10)$$

Furthermore, considering that $\Delta t = 1/f_s$, where f_s is the sampling frequency, using the normalized angular frequency Ω, and, combining Eq.(7) and Eq.(8) , we obtain Eq.(11)

$$\sin\phi_n = \frac{1}{A_1\cdot A_2\cdot\Omega}|\vec{P_{n-1}}\times\vec{P_n}| \quad (11)$$

We also add an adjustment to the above partial area calculation illustrated in Fig.3. The exact areas of the arc and the triangle are; $S_{arc} = r^2\theta$ for the area connected by the arc, and $S_{vec} = r^2\sin\theta$, approximated by the vector product. The partial area obtained by the vector product is slightly smaller than the actual area. In order to obtain the correct value of the partial area ΔS, An adjustment constant $\frac{\Omega}{\sin\Omega}$ must be multiplied. Finally, we obtain Eq.(12);

$$\sin\phi_n = \frac{1}{A_1\cdot A_2\cdot\sin(\Omega)}|\vec{P_{n-1}}\times\vec{P_n}| \quad (12)$$

Only two trajectory locations $\vec{P_{n-1}}$ and $\vec{P_n}$ can produce the instantaneous phase difference $\sin\phi_n$ by using Eq.(12). Furthermore, if we assume that we are measuring a quadrature signal, mostly generated by a Hilbert transform, then $\sin\phi = 1$, $A_1 = |P_{n-1}|$ and $A_2 = |P_n|$. Consequently, Eq.(13) is derived for very simple instantaneous frequency calculation, which is surprisingly equivalent to the definition of the cross product.

$$\sin\Omega_n = \frac{|\vec{P_{n-1}} \times \vec{P_n}|}{|\vec{P_{n-1}}||\vec{P_n}|} \tag{13}$$

2.4. Estimating Frequency by Frequency Deviation

In this section, we describe how to exactly calculate Ω from the measured phase shift $\sin\phi_c$ without approximation. It is generally difficult to determine the inverse phase transfer function $\Omega = \phi^{-1}(\phi_c)$ In order not to use an approximation, we introduce the widely known so-called Weierstrass substitution [5]. By replacing $x = \Omega K$ and $t = \tan(x/2) = \tan(\Omega K/2)$, we obtain $\sin(\Omega K)$ and $\cos(\Omega K)$ as Eq.(14).

$$t = \tan(x/2), \quad \sin(x) = \frac{2t}{1+t^2}, \quad \cos(x) = \frac{1-t^2}{1+t^2} \tag{14}$$

First, we change the representation of the phase angle $\sin\phi_c$ to tangent angle q_0.

$$q_0 = \frac{\sin\phi_c}{\sqrt{1-\sin^2\phi_c}} \tag{15}$$

Using Eq.(2), we obtain the following equation.

$$q_0 = \tan(\phi(\Omega)) = \frac{Im(H)}{Re(H)} = \frac{-a\frac{2t}{1+t^2}}{1-a\frac{1-t^2}{1+t^2}} \tag{16}$$

By solving Eq.(16), we obtain the quadratic equation Eq.(17) to obtain the final answer t.

$$q_0(1+a)t^2 + 2at + q_0(1-a) = 0 \tag{17}$$

Thus, we obtain two possible expression of t as:

$$t = \frac{a \pm \sqrt{a^2 - q_0^2(1-a^2)}}{q_0(1+a)} \tag{18}$$

x is obtained as:

$$x = 2 \cdot \arctan(t) \tag{19}$$

When the frequency given to the comb filter is around the resonant frequency (for odd harmonics), x becomes around π. In our parameter set up, a has a negative value around -0.8. We show the equations Eqs.(20) to determine the measured frequency.

$$\begin{aligned} d &= sign(x) - \frac{x}{\pi} \\ f &= f_0 \cdot (1+d) \end{aligned} \tag{20}$$

We can obtain the frequency deviation d by obtaining x. Note that only two sets of signals from the comb filter produce an instantaneous frequency.

3. MOVING VECTOR ESTIMATION BY DOPPLER SHIFT

This section describes the estimation of the moving vectors of a target by using the Doppler-shifted frequency from the target. A frequency deviation of less than 1 Hz was directly measured using PRIMO.

3.1. Doppler Shift and Vector Definition

The Doppler shift is expressed by Eq.(21), where f_0 is the sound source frequency, v_0 is speed of sound ($v_0 = 331.5 + 0.61t$). and v is the speed of the target.

$$f = \frac{v}{v_0 - v} f_0 \tag{21}$$

We define two direction vectors $\vec{r_1}$ and $\vec{r_2}$ from two microphones Mic.(L) and Mic.(R) pointing to the target P, as shown in Fig.5. The

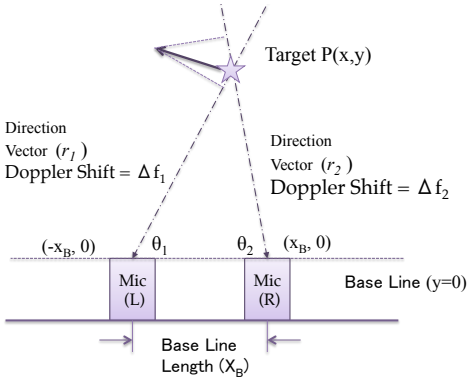

Fig. 4. Tracking Model

baseline $\vec{B}$ is the line between the left (L) and right (R) microphones. When the target location is $\vec{P_n}$ and the base locations $\vec{B_1}$,$\vec{B_2}$ are expressed by $\vec{B_1} = (-X_B, 0)$, $\vec{B_2} = (X_B, 0)$, the direction vectors $\vec{r_1}, \vec{r_2}$ are as Eq.(22), where the baseline is $\vec{B} = \vec{B_2} - \vec{B_1}$.

$$\vec{r_1} = \vec{P} - \vec{B_1}, \qquad \vec{r_2} = \vec{P} - \vec{B_2} \tag{22}$$

The angle $\theta_k (k = 1, 2)$ from the baseline is obtained by Eq.(23).

$$\sin\theta_k = \frac{|\vec{B} \times \vec{r_k}|}{|\vec{B}||\vec{r_k}|}, \qquad \cos\theta_k = \frac{\vec{B} \cdot \vec{r_k}}{|\vec{B}||\vec{r_k}|} \tag{23}$$

3.2. Moving Vector and Location Estimation

We can estimate the moving vector from the Doppler-shifted frequency using Eq.(24), where the frequency deviation representation $F_d = \Delta f / f_0$. Note that positive F_d means that the target is approaching to the sound source.

$$v_k = \frac{-F_{d(k)}}{1 + F_{d(k)}} \cdot v_0 \tag{24}$$

The Doppler shift is affected only along the Direction Vector. Therefore the moving vector and the location are given by Eqs.(25).

$$\begin{aligned} \frac{d}{dt}\vec{r_k} &= v_k \cdot [\cos\theta_1, \sin\theta_1]^t \\ \frac{d}{dt}\vec{P} &= (\frac{d}{dt}\vec{r_1}) + (\frac{d}{dt}\vec{r_2}) \end{aligned} \tag{25}$$

The location $\vec{P_n}$ can be obtained by integration of $\frac{d}{dt}\vec{P}$ given by Eq.(26). Note that this estimation requires the initial value P_0. Basically measuring the Doppler-shifted frequency only can detect the velocity. The explicit angle difference between $\vec{r_1}$ and $\vec{r_2}$ is estimated experimentally as follows.

$$\vec{P_n} = \vec{P_{n-1}} + h \cdot \frac{d}{dt}\vec{P_{n-1}}, \quad \text{where} \quad h = \frac{1}{f_s} \tag{26}$$

4. EXPERIMENTS

4.1. Experiment Overview

Figure 5 illustrates the tracking model and Fig.6 is a photograph of the pendulum, speaker and two microphones. We examined the velocity and the location estimation. We used the pendulum oscillation and determined the fundamental period and initial speed of the oscillation. A speaker was placed at the end of the pendulum and was driven using a function generator (FG) with a fixed frequency ($f_0 = 441.000,000$ Hz) sine wave. Two microphones (L and R) simultaneously measured precise frequency movements with the Doppler shift $\Delta f_1, \Delta f_2$. The length of the pendulum was 76 cm. The baseline length X_B was 2 cm and the minimum height was 10 cm. The diameters of the speakers were 10 cm.

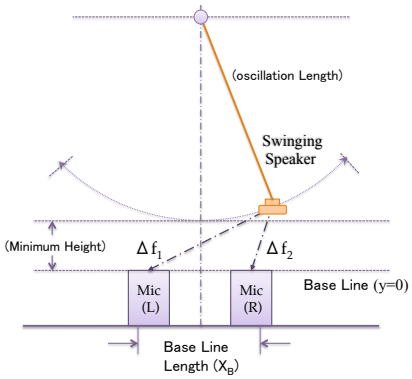

Fig. 5. Tracking Model

Fig. 6. Pendulum/Speaker/Microphones

4.2. Experimental Results

4.2.1. Evaluation of Fundamental Accuracy

This section illustrates the evaluation results of the fundamental accuracy of PRIMO. Figure 7 (a) shows that PRIMO detected an accurate frequency with a resolution of several μHz. The testing signals were generated using an FG (Agilent 33522A), which refers to the external reference clock from the Rubidium (Rb) oscillator. Figure 7 (b) shows a measurement example of extremely slow and small frequency deviation movement.

4.2.2. Calibration for Tracking

This section discusses how PRIMO can measure two FM-modulated signals as if the target Doppler-shifted signals are given to the two microphones. Figure 8 shows the measured data from using PRIMO.

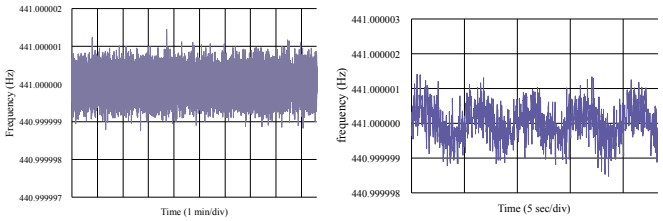

(a) The frequency resolution by calibrated Rb. Osc.

(b) Extremely small frequency deviation detection

Fig. 7. Accuracy Evaluation

Two differently FM-modulated signals were produced by the FG. The evaluation conditions were based on the estimated swinging parameters of the pendulum. The center frequency f_0 was 441.000,000 Hz, and the signals were FM-modulated by a sine wave. The modulating frequency was 0.5 Hz for the Left Signal and 1.0 Hz for the Right Signal. The modulation frequency ratio was $1:2$. The frequency deviations Δf_1 and $\Delta f_2 = 100$ mHz. PRIMO exhibited a 23.2-msec time resolution. The frequency deviation and modulating frequency were precisely measured, as shown in Fig.8.

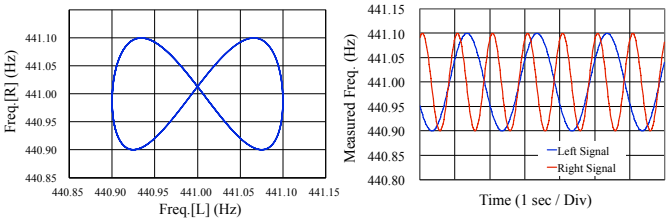

(a) Frequency Deviation Scatter Plot of two FM-signals

(b) Actually Measured Frequencies

Fig. 8. Calibration for Tracking

4.2.3. Evaluation of Noise Robustness

This section describes the noise robustness of PRIMO. In this implementation, a pre-processing Bandpass Filter (BPF) was located in front of the comb filter to extract the target frequency. Table 1 lists the frequency errors described by the standard deviation (SD) for different signal-to-noise ratio (SNR) conditions. The graph is shown in Fig.9. The testing frequency $f_0 = 441.000,000$ Hz was used precisely referenced to the Rb oscillator. In general, poor SNR causes less frequency resolution. However, PRIMO is capable of extracting the target signal at SNR=0 (dB) in the order of a several-mHz measurement error.

Table 1. Noise Robustness

Noise Level	SNR (dB)	Measured Freq.(Hz)	SD of Error. (Hz)
14.28	-23.1	441.0150823	2.32E-02
12.5	-21.9	441.011,5885	2.85E-02
10.0	-20.0	441.006,9953	1.35E-02
1	0.0	441.000,0707	1.11E-03
0.1	20.0	441.000,0008	1.11E-04
0.01	40.0	441.000,0000	1.11E-05

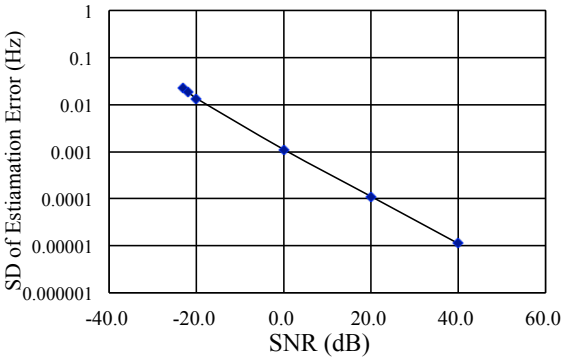

Fig. 9. Noise Robustness

4.2.4. *Tracking the Oscillating Sound Source*

During this experiment, we tracked the moving sound source by measuring the Doppler-shifted frequency. Figure 10 shows the measured frequency deviation of the moving sound source on the oscillating pendulum. The two microphones detected the Doppler-shifted frequency at each location. The frequency deviation Δf_1 was measured using the left microphone (Mic. L), and Δf_2 was measured using the right microphone (Mic. R). Note that the speed of the sound source was momentarily zero when the speaker transits at both ends of the pendulum oscillation. The trajectory on Fig.10 transits on the origin at that moment. The sign of the frequency deviations $\Delta f_1, \Delta f_2$ was either positive or negative. The trajectory in the 1^{st} quadrant means that the target was approaching the microphones, the trajectory in the 3^{rd} quadrant means that the target was moving away from the microphones, and the trajectory in the 2^{nd} or 4^{th} quadrant means that the target was quickly passing between the two microphones.

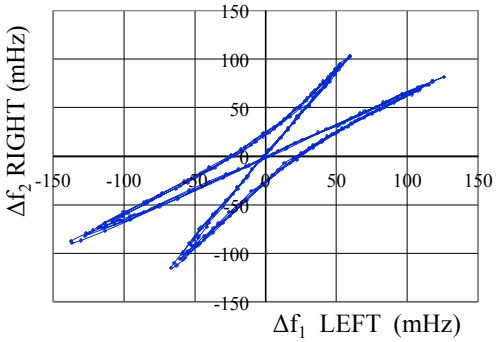

Fig. 10. Tracking the Oscillating Sound Source

4.2.5. *Velocity and Location Estimation with the Phase Angle*

Measuring the exact instantaneous physical location of the sound source requires mechanical experiments. Alternatively, we measured the direct phase difference between the two microphones. Figure.11 shows two types of phase angle movements data. One was directly measured using PRIMO and the other was estimated using actually measured frequency deviations Δf_1, and Δf_2. The two phase differences results were mostly equivalent, which follows the oscillation displacement of the pendulum at each moment.

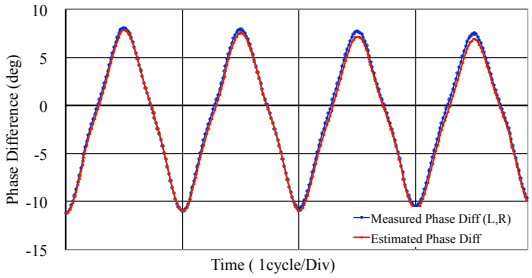

Fig. 11. Phase Angle Measurement

4.2.6. *Error in near distance detection*

The estimated phase difference in the Doppler shift from the two microphones shown in Fig.11 did not always correspond to the actual direction. When the curve of the phase angle crossed zero degree, the curve became rather bent. This indicates that the sound is not radiated from an ideal point source. In the experiment, the size of the speaker was too large (shown in Fig.6); therefore, when the speaker on the pendulum was passing above the baseline at a near distance, the radiation source seemed to no more be a point source. No sufficient phase difference was generated during that movement.

5. CONCLUSIONS

We proposed a sound source tracking method, using a Doppler-shifted frequency measurement, called PRIMO, and explained the principle. The evaluation data shows that PRIMO exhibits sufficient level time-frequency resolution for Doppler-shifted frequency measurement and can measure a precise frequency shift even under noisy conditions. The velocity and location of the moving sound source can be directly measured using Doppler-shifted frequencies and with the directly measured phase angle.

6. REFERENCES

[1] Yiu-Tong Chan and F. Jardine, "Target localization and tracking from doppler-shift measurement," in *Proc.* IEEE Journal of Oceanic Engineering, 1990, vol. 15-3, pp. 251–257.

[2] B. Ristic and Alfonso Farina, "Joint detection and tracking using multi-static doppler-shift measurements," in *Proc.* ICASSP 2012, 2012, pp. 3881–3884.

[3] K. Nakadai, H. Nakajima, M. Murase, S. Kaijiri, T. Nakamura K. Yamada, Y. Hasegawa, H. Okuno, and H. Tsujino, "Robust tracking of multiple sound sources by spatial integration of room and robot microphone arrays," in *Proc.* ICASSP 2006, 2006, vol. 4, p. 932.

[4] Frederick J. Rasmussen, "Frequency measurements with the cathode ray 0scilograph," *American Institute of Electrical Engineers, Transactions*, vol. XLV, pp. 1256–1265, Jan 1926.

[5] Michael Spivak, *Calculus*, Cambridge University Press, Cambridge, 2006.